

Article

Biofabrication of Silver Nanoparticles Using Teucrium Apollinis Extract: Characterization, Stability, and Their Antibacterial Activities

Wanisa Abdussalam-Mohammed ^{1,*}, Laila Mohamed ², Mohammed S. Abraheem ¹,
Mohmeed M.A Mansour ³ and Akram Mansour Sherif ⁴

¹ Chemistry Department, Faculty of Science, Sebha University, Sebha P.O. Box 18758, Libya

² Chemistry Department, Faculty of Science, University of Tripoli, Tripoli P.O. Box 13662, Libya

³ Chemistry Department, Faculty of Science, University of Al-Jufra, Al-Jufra P.O. Box 61602, Libya

⁴ Libyan Biotechnology Research Center, Tripoli P.O. Box 30313, Libya

* Correspondence: wan.ahweelat@sebhau.edu.ly

Abstract: Medical science has paid a great deal of attention to green synthesis silver nanoparticles (AgNPs) because of their remarkable results with multidrug-resistant bacteria. This study was conducted on the preparation of AgNPs, using the teucrium apollinis extract as a reducing agent and a capping ligand. The AgNP produced was stable in room condition up to 10 weeks. The AgNP was characterized using UV-visible absorption spectroscopy (UV-Vis), attenuated Fourier transform infrared (ATR-FTIR), transmission electron microscopy (TEM), and dynamic light scattering (DLS). The study confirms the ability of teucrium apollinis to produce AgNPs with high stability. The influence of pH was studied over a pH range of (2–12) on the stability of synthesized AgNPs. The best value of pH was 7.2, where AgNP showed a good stability with high antibacterial activity against *Pseudomonas aeruginosa*. AgNP synthesis is confirmed by a strong peak in the UV-Vis due to surface plasmon resonance (SPR) at 379 nm. Based on TEM findings, monodispersed AgNP has a spherical shape with a small size of 16 ± 1.8 nm. In this study, teucrium apollinis extract was used for the first time, which could be a good environmental method for synthesizing AgNP, which offers a possible alternative to chemical AgNPs.

Keywords: teucrium apollinis; *Pseudomonas aeruginosa*; silver nanoparticles; pH; stability; aggregation; antibacterial activities



Citation: Abdussalam-Mohammed, W.; Mohamed, L.; Abraheem, M.S.; Mansour, M.M.A.; Sherif, A.M. Biofabrication of Silver Nanoparticles Using Teucrium Apollinis Extract: Characterization, Stability, and Their Antibacterial Activities. *Chemistry* **2023**, *5*, 54–64. <https://doi.org/10.3390/chemistry5010005>

Academic Editor: Edwin Charles Constable

Received: 19 November 2022

Revised: 8 December 2022

Accepted: 28 December 2022

Published: 2 January 2023



Copyright: © 2023 by the authors. Licensee MDPI, Basel, Switzerland. This article is an open access article distributed under the terms and conditions of the Creative Commons Attribution (CC BY) license (<https://creativecommons.org/licenses/by/4.0/>).

1. Introduction

Due to their distinct chemical and physical characteristics, silver nanoparticles (AgNPs), as one type of metal nanoparticle, are increasingly exploited for industrial and medical uses [1]. Silver nanoparticles possess a wide variety of antibacterial, antifungal, and antiviral properties. The potency of AgNPs as an antibiotic is a result of their different mechanisms of action, which attack microorganisms in multiple structures at the same time, and provide them with the capability to kill different types of bacteria [2]. Silver nanoparticles can change the composition of cell membranes and potentially result in cell death when they invade the walls of bacterial cells [2]. Their large surface-area-to-volume ratio and nanoscale size both contribute to their effectiveness [3]. In addition, the contact area and interaction of the nanoparticle with the medium are influenced by the nanoparticle's size. Smaller NPs have been found to dissolve more quickly in various environments, releasing silver ions in the process, which may play a significant role in the antibacterial impact of nanoparticles [2].

Gram-negative bacteria, as they are known, are among the main agents in a nosocomial infection, contributing to an increase in patient mortality. *Pseudomonas aeruginosa* is one of the Gram-negative bacteria that is highly susceptible to genetic modifications, causing a

resistance to antibiotics and leading to impaired or immunocompromised patients, as a result of its ability to survive in harsh environments [4].

Based on previous studies [2], the physicochemical properties of AgNPs, including size and surface, have been found to be responsible for allowing AgNP to interact with cell membranes and directly affect intracellular components.

The selection of ligands is of the highest importance for the colloidal stability and sizes controlling of the NPs. According to Balkrishna et al., the size-dependent bactericidal properties of green synthesized AgNPs of a small size ($\sim 10 \pm 2$ nm), exhibit more antibacterial activity compared with larger sizes [5].

It is well known that AgNPs synthesized using green methods are preferred as a co-environment compared to chemically synthesized AgNPs [6].

As a result of its many benefits, such as simplicity, eco-friendliness, and low cost, the green synthesis of metallic nanoparticles has recently arisen as a new and intriguing field of study. When compared to chemically manufactured NPs, the NPs produced through green synthesis are typically stable, simple to prepare, do not require heating or reducing agents, and are also quite safe [7,8].

In addition, the reagents used in green synthesis are non-toxic. This form of synthesis also requires fewer reagents because plant extracts serve as both reducing and stabilizing agents. The reaction frequently takes place in a single step, and it is very rapid and efficient [9].

The surface chemistry, shape, size, size distribution, particle morphology, particle composition, capping agent, agglomeration, dissolving rate, particle reactivity in solution, effectiveness of ion release, and cell type are some of the variables that affect the biological activity of AgNPs [1]. This study illustrates the bioactivity of biocompatible AgNPs dispersed in an aqueous solution and capped by *teucrium apollinis* extract. The plant in this paper was chosen based on its therapeutic applications [10]. We noted that this extract is used to stabilize and enhance the antibacterial properties of Ag NPs.

2. Materials and Methods

The primary requirement for the synthesis of AgNPs is silver nitrate (AgNO_3), which is purchased from Sigma-Aldrich and used without any further purification.

2.1. Green Synthesis of AgNP by Using *Teucrium Apollinis* Extract

In April 2021, at the flowering stage, *teucrium apollinis* leaves were taken from the Slop Mountains of Ras El-Hilal, Cyrenaica area, Libya.

2.1.1. *Teucrium apollinis* Extraction Procedure

The leaves of the plant were washed and allowed to dry in the shade. The dry plant was then ground into a soft powder. Petroleum ether (40–60 °C) and the Soxhlet apparatus were used to extract this powder. The plant extract used as a capping ligand and reducing agent in this study was obtained as a solid after the solvent was evaporated using a rotary evaporator at 40 °C.

2.1.2. Synthesis of Silver Nanoparticles

20 mL of distilled, deionized water were used to dissolve AgNO_3 (0.0065 g, 0.038 mol). Next, 0.0095 g of extract plant (dissolved in 5 mL of distilled water) was added step by step to the last mixture and stirred for 3 h. The vigorous stirring was kept up for a further 2 h, as evidenced by the appearance of a light yellowish-green tint that confirmed the reduction of Ag^+ ions to Ag^0 , as described in Figure 1. The sample was centrifuged three times and re-dispersed before being rinsed with EtOH/distilled H_2O (1:2) and used for the subsequent characterizations. The samples were stored in accordance with standard laboratory procedures.



Figure 1. Process of green synthesis of AgNP using *Teucrium apollinis* extract as coating and reducing agents at the same time. A plant extract of (5 mL) was added stepwise to silver nitrate solution ($\text{AgNO}_3/\text{H}_2\text{O}$) with vigorous stirring. The progress of the formation of AgNPs can be observed through visual color changes or by using UV-Vis.

2.2. UV-Visible Spectroscopic Investigation

AgNP production was detected by the appearance of a yellowish-brown color, which typically has wavelengths between 350 nm and 450 nm in the UV-Vis spectra [11].

The AgNPs composition was investigated by scanning the AgNPs suspension with an Evolution™ 300 UV-Vis spectrophotometer, with spectra ranging from 200 to 800 nm. Distilled water was used as a blank. Measurements were carried out in quartz cuvettes (1 cm light path).

Study of the Silver Nanoparticle's Stability

The durability of metal nanoparticles over time is one of the crucial aspects of their suitability for use. Figure 2 displays the stability of AgNPs up to 10 weeks. The intensity of the plasmon resonance bands was raised as time was increased, showing that large sizes are created after around 10 weeks, and excluding any possibility of aggregation. As can be seen, the absorbance of AgNP, initially measured at 379 nm, increased to 406 nm after 10 weeks. According to Czechowska-Biskup, R et al. [12], changes in absorbance values suggest that the reduction process will continue to take place [12].

Based on later investigation, the position of the localized surface plasmon resonance (LSPR) spectrum from each of the NPs normally undergoes a very uniform red shift with increasing local index; however, it was found that the amount of red shift per index increase varies depending on the shape of the NP. For example, the spectral peak that occurs in triangular nanoparticles exhibits a significantly larger red shift than that of spherical nanoparticles [13]. In the same way, the SPR peak typically migrated to a higher wavelength region. Since more AgNPs are expected to form at higher concentrations, this can be attributed to NP aggregation [14].

In our result, spherical AgNP offered a small red shift which, indicative of an effective plant extract, indicated a high stable AgNP and the size became a little bigger after 10 weeks after being prepared.

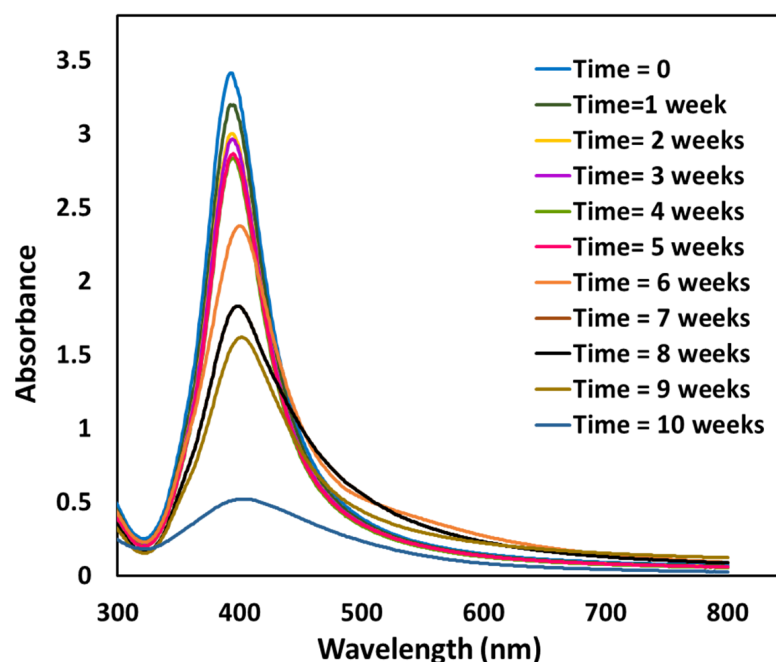


Figure 2. UV-Vis spectra of colloidal AgNPs over a period of 10 weeks. The peaks of absorption were at a wavelength of 379 nm and 406 nm at the initial time (time = 0) and after 10 weeks, respectively. With more time passing, the dispersed silver nanoparticles' sizes seemed to grow larger (bigger red shift noted after 10 weeks).

According to additional investigations, the agglomeration of smaller particles results in the production of larger particles as the λ_{max} value shifts towards higher wavelengths with increasing duration [15]. However, teucrium extract offered high stability to AgNP due to its chemical composition, which includes phenols, flavonoids, and alkaloids, which have a high affinity towards the surface of NP [16]. The AgNP produced by this extract (see Figure 2), showed a relatively large size in this study only after 10 weeks. The choice of ligands used in nanoparticle synthesis can change their final sizes and shapes as well as improve their colloidal stability [17].

It is often mentioned that the absence of peak in the region 335 and 560 nm in UV-Vis spectra is taken as a sign that AgNPs are not aggregated [18], and these indicators are in agreement with our results.

2.3. pH Stability Study of AgNPs

The stability of the synthesized AgNP was studied by changing the conditions of pH values. The size of the AgNPs was controlled by adjusting the pH levels of the reaction system. For instance, at higher pH values, smaller AgNPs were produced in comparison to lower pH values. This variation can be explained by the variations in the reduction rate of the precursors [19].

In this study, the impact of pH on the green synthesis of AgNPs is examined. Figure 3 displays the absorption spectra at various pH levels (1.7 to 12.1). AgNP is systematically tested to see how adding HCl or NaOH (5 μL to 25 μL , 0.1 M) affects the character of NP, as seen in Figure 3. The AgNPs, dispersed in aqueous solution, were prepared at pH 7.2 values. However, with the pH changing, the AgNP displayed different surface plasmon resonance (SPR) behavior. This resulted from changes in the size and size distribution of the AgNPs, which were confirmed earlier [15,20].

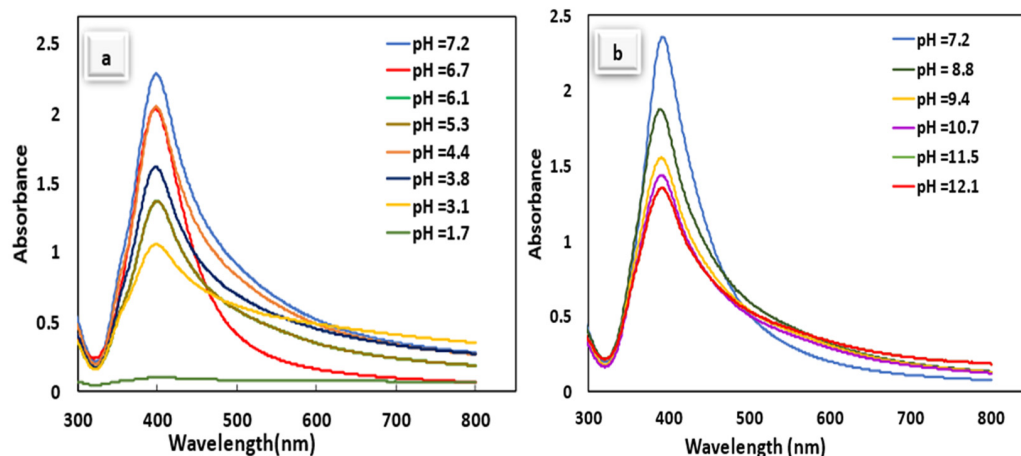


Figure 3. UV-Vis data collected across the pH range produced by adding HCl, 0.1 M (a) or NaOH, 0.1 M (b) to aqueous AgNP functionalized by Teucrium apollinis extract. The SPR shifting from 397 nm at pH = 7.2 to 408 nm and 401 nm at pH 3.1 and pH 12.1, respectively.

pH Study of the Stability of Teucrium Apollinis-AgNPs- in Acid and Basic Conditions of 0.1 M HCl and 0.1 M NaOH

It has been demonstrated that pH alternation causes a change in the shape and size of produced AgNPs. As is known, the shape and size of the NP affect the cellular uptake in addition to its antibacterial effect [21].

Some studies illustrated that high acidic and alkaline pH cause a reduction in the growth of bacterial cells. For instance, the antibacterial activity of ZnO NPs was influenced by pH values, and higher antibacterial activity was observed at acidic pH levels (pH = 4–5) [22]. In the present study, AgNP had a highly bacterial effect at pH 7.2. Our findings supported the possibility that different pH levels could be responsible for the differences in AgNP stability, size, and variations biological effects.

It is worth note that increasing the pH value leads to generate spherical nanoparticles, whereas at lower pH, rods and triangular particle forms are formed. This difference is due to the poor balance between the processes of nucleation and growth [19]. As clearly shown in Figure 3, the absorbance peak shifted towards longer wavelengths with an increase in pH values, which indicated an increase in the particle size, as reported in the literature [14].

The size of the silver nanoparticles in this paper was controlled by changing the pH values of the reaction system. The pH was adjusted to 7.2, and smaller-size AgNPs were produced in comparison to high and low pH values. This has been confirmed by UV-Vis absorption data. For example, the AgNP has a surface plasmon peak at a wavelength of 397 nm at pH 7.2. Nevertheless, it is increased to 422 nm when the pH is raised to pH 12.1. The same change was shown at a low pH (pH 3.1) value. This change can be attributed to the difference in the chemical and physical properties of AgNPs [15]. Figure 3 confirmed that changing the pH of the solution to below 5 or above 9 causes the formation of larger nanoparticles.

3. Results

The current study showed how AgNP can be produced by reducing aqueous AgNO₃ with Teucrium apollinis extract without using any additional reducing agents.

3.1. TEM Results

The ideal tool for chemical and structural characterization at the nanoscale is the transmission electron microscope (TEM). It is simple to generate imaging, diffraction, and microanalytical data. which may then be integrated to provide extensive insights into the characteristics and behavior of nanostructured materials [23].

TEM is performed to study the morphology and size of AgNPs. Both the examination of the particles and the creation of the TEM micrographs were carried out using a JEOL 2100 field emission gun transmission electron microscope (FEG TEM) set at 100 KV. In general, the size distribution of AgNP was obtained by counting and measuring over 160 silver nanoparticles. The deposition method was used to prepare the samples for TEM analysis. A drop of a dilute colloidal of AgNP was applied and suspended on a Holey carbon-coated copper grid. The grid was then dried at room temperature.

It was shown that the three key components for AgNPs in medical applications are monodispersing, small size, and spherical structure [24].

The TEM results showed monodispersed AgNP, with most of the prepared AgNP having radii less than 17 nm, and about 40% having radii between 18 and 19 nm.

It is clear that the uniform spherical shape could be seen in the TEM image and AgNP did not show any aggregation or agglomeration, which confirms the successful synthesis of AgNP using plant extracts as the capping/reducing agent (see Figure 4), and it is suggested as a viable option for regulating the size and shape of NPs.

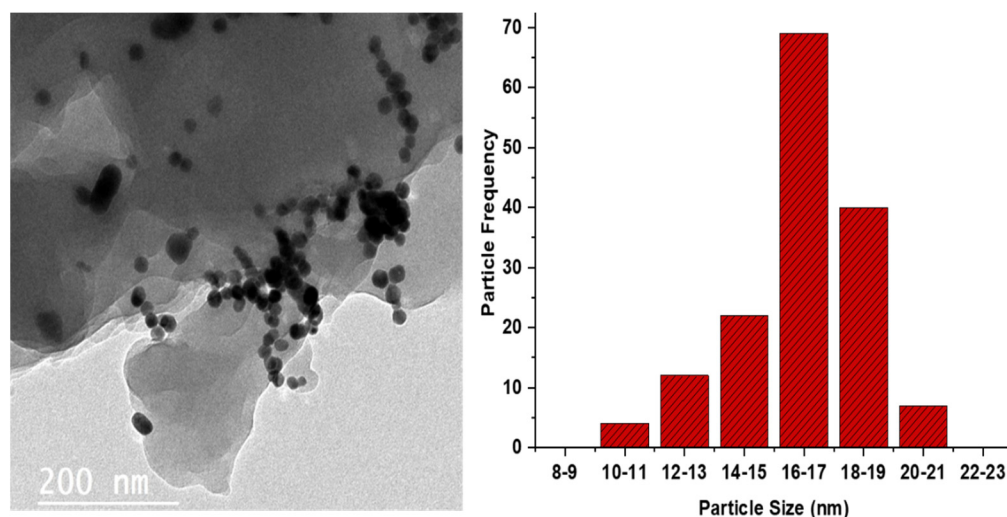


Figure 4. TEM micrographs of AgNPs synthesized by *Teucrium apollinis* extract as protecting and stabilized ligands. AgNP is formed in a spherical shape with a 16 ± 1.8 nm size.

3.2. Dynamic Light Scattering (DLS) Analysis

DLS was carried out using a (Zetasizer Nano ZS (Malvern Instruments Ltd., UK) to evaluate both the size and size distribution of NPs. The AgNP sample was analyzed after being diluted in distilled water (1:1) at 25 °C. Sample measurements were performed in triplicate. DLS analysis was used to get further details on the particle size distribution. The DLS size distribution histogram of Ag NPs was illustrated in Figure 5. The findings indicate that the size distribution ranges of compatible Ag NPs are from 20 nm to 41 nm, and this range corresponds with the outcome of a TEM image. The average particle size distribution was calculated to be 30 ± 2.2 nm.

In this investigation, where AgNPs remained a monodisperse and stable event 10 weeks after preparation time, the results of DLS of AgNPs and TEM confirmed each other. Due to the presence of phenolic chemicals in the extract plant, the size of the AgNPs seems large. This confirms that ligands have the ability to effect of modifying the growth phase, which is similar to previous research results [25].

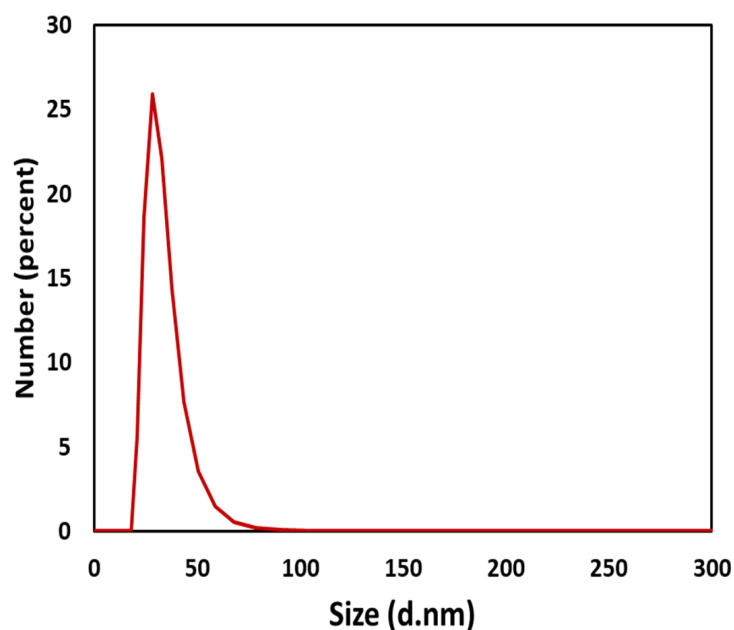


Figure 5. DLS diagrams of AgNPs functionalized by extract of *Teucrium apollinis*.

3.3. Attenuated Total Reflection Fourier Transform Infrared Spectroscopy (ATR-FTIR)

ATR-FTIR analysis was performed to confirm the functional groups of green synthesized AgNPs by ATR-FTIR (Bruker Tensor 27, Germany). The spectral absorbance of samples was recorded in the range of ATR-FTIR spectra of the AgNPs and plant extract, which were recorded in the $400\text{--}4000\text{ cm}^{-1}$ range at a resolution of 4 cm^{-1} . The background spectrum was recorded before each analysis. To measure and examine the spectra, origin software (version 7.5) with a Peak-Fitting Module (PFM) was employed.

Figure 6 compares the ATR-FTIR spectra of *Teucrium apollinis* extract and AgNPs functionalized by the same plant extract. AgNP is represented by the first curve (black line). The IR bands of a pure stabilized ligand (*Teucrium apollinis* extract) are shown in the second curve (red line). According to a previous study, ligands containing carboxyl groups were adsorbed onto the nanoparticle surface through their carboxyl groups [25].

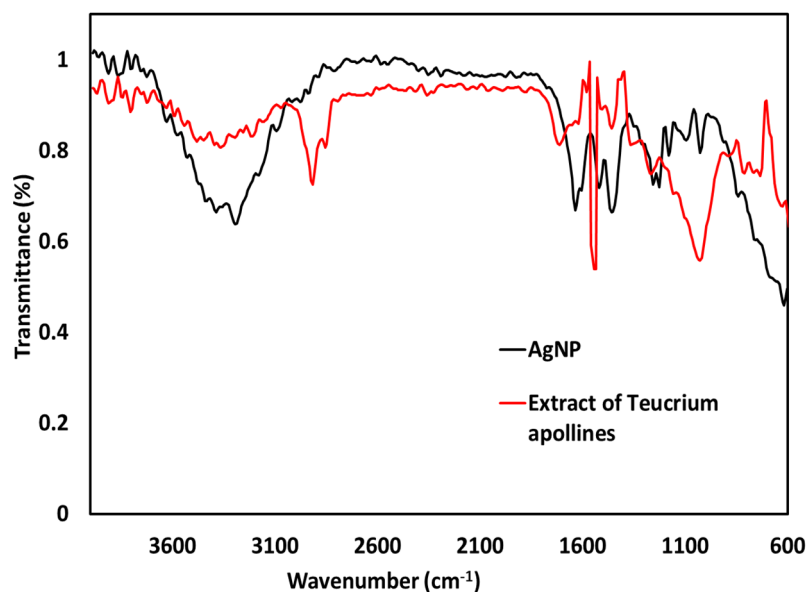


Figure 6. Comparison between extract of *Teucrium* and AgNP functionalized by the same extract.

The (C=O) peak for *teucrium apollinis* appeared at 1705 cm^{-1} , shifting to 1650 cm^{-1} in the case of AgNP functionalized by this ligand, as shown in Figure 6. The peak at 2917 cm^{-1} in the *teucrium apollinis* extract curve is due to an aromatic ring (phenyl group). This peak is shifted to 3116 cm^{-1} in the AgNP sample, confirming the interaction between them. According to Figure 6, the broad peak in the range of $3100\text{--}3500\text{ cm}^{-1}$ in the AgNP curve spectra shows the presence of –OH groups. The IR consequences indicate the presence of carboxyl groups [(–C=O), and OH] groups, which represent the presence of sugar, proteins, and amino acids on the surface of the generated AgNPs and are responsible for stabilizing AgNPs [26]. The IR result of AgNP has also shown peaks of absorption bands at 1380 cm^{-1} and 890 cm^{-1} , representing the presence of Ag–O bond that is consistent with earlier research [14]. It can be summarized that the production of AgNP is caused by the phenyl, hydroxyl, and carbonyl groups in plants, which donate an electron to the silver ions [14].

3.4. Antibacterial Activities of Silver Nanoparticles

Numerous studies have examined the detrimental effects of specific microbe kinds on wound healing; these bacteria are frequently cited as the root cause of delayed wound healing. *Pseudomonas aeruginosa* is one of the most popular pathogens causing these infections. To treat or prevent wound infections, antimicrobial medications such as silver compounds, iodine compounds, acetic acid, and chlorhexidine are frequently used [27].

Nanoparticles are widely used today, particularly in the most advanced scientific materials. Silver nanoparticles, one of the most popular antimicrobial materials, have been generally used in the textile industry and medical engineering [1].

Furthermore, the majority of infections in newborns are thought to be caused by *Pseudomonas aeruginosa*, which presents considerable therapeutic hurdles for treating these illnesses [28]. For this reason, this kind of bacteria was selected as a model in this investigation due to its prevalence and significance in human diseases [29].

In the present study, the antibacterial activity of AgNPs against *Pseudomonas aeruginosa* bacterial strains was examined. Growth studies with optical density (OD) measurements were performed to evaluate the antibacterial activity of AgNPs in a quantitative manner. The approach was applied using a specified procedure [30]. At $37\text{ }^{\circ}\text{C}$, the samples were incubated for 6 h. Using a UV-Vis spectrophotometer (Jenway model 6305, UK), the optical density at 600 nm (OD600) of the samples was measured after various incubation times (0, 1, 2, 3, 4, 5, and 6 h). In order to compare the antibiotic (imipenem ug) with the AgNP sample, the generated data was evaluated using the GRAPHPAD PRISM V5.00 program, which employs the ANOVA test ($p < 0.05$). Samples containing only bacterial strains and culture medium (without AuNPs) under the same conditions were used as the blank control.

The antibacterial activity of the generated AgNPs against the multidrug resistant *Pseudomonas aeruginosa* is shown in Figure 7. At the beginning of the incubation, the bacteria continued to proliferate while exposed to AgNPs (for 1–2 h). However, its growth drastically decreased after 2 h (4–6 h). This is due to the presence of phenolic compounds in the *teucrium* extract. As with previous data, due to its strong affinity for bacterial cells, it can more easily connect with their membrane and inhibit them [31]. Studies on the bioactivity of green-made AgNPs have shown that these AgNPs were more effective than synthetic chemical AgNPs in responding as a microbiological growth inhibitor against the bacterium *Pseudomonas aeruginosa* [31]. According to our efficacy findings, the *teucrium apollinis* extract-AgNP is quite effective against *Pseudomonas aeruginosa*, as a Gram-negative microorganism. This can be explained by the easier entry of smaller nanoparticles into the cell wall of Gram-negative bacteria, which has a single peptidoglycan layer and a distinct outer membrane layer [32]. The findings in this study are in agreement with previous reports that indicate greater activity of silver nanoparticles against *Pseudomonas aeruginosa* [4].

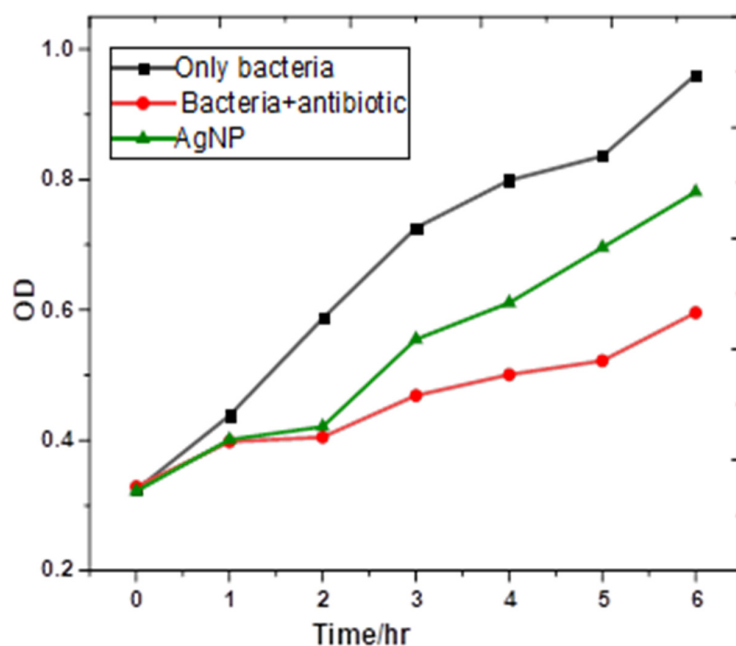


Figure 7. The growth curves of *Pseudomonas aeruginosa* after exposure to AgNP functionalized by Teucrium extract are displayed, along with a comparison of Ag-NPs to an antibiotic (imipenem 10 µg, red curve) over the duration of 1–6 h ($p < 0.05$). The control sample (black curve) contains only bacteria, without AgNPs.

4. Conclusions

Colloidal silver nanoparticles were prepared according to the green synthesis method, in which the teucrium apollinis extract was used as a reducing as well as a stabilizing agent. This plant extraction reduced Ag (I) to Ag (0) and provided the AgNPs with excellent stability, which is demonstrated by using UV-Vis, TEM, and DLS results.

In addition, AgNP did not show any decomposition characteristics, such as particle growth or instability. The effect of the pH (1.7–12.1) on the AgNP was carried out and showed the best value for good stability was (pH = 7.2). Stability was observed for up to 10 weeks under normal laboratory conditions. According to the TEM and DLS results, the AgNP has a spherical shape with an average size of 16 nm.

The bioactivity of AgNP stabilized by teucrium apollinis was applied against *Pseudomonas aeruginosa* and showed good results. This type of size-controlled, environmentally friendly AgNP can be made in an easy, cost-effective way, and may be suitable for the formulation of new kinds of antimicrobial materials for biomedical and pharmaceutical applications. However, further research in vivo is required to determine the toxicity of this type of nanomaterials.

Author Contributions: Conceptualization, W.A.-M., Methodology, W.A.-M. and M.S.A., Writing an original draft, W.A.-M. Writing-review and editing, W.A.-M., L.M., M.M.A.M. and A.M.S. All authors have read and agreed to the published version of the manuscript.

Funding: This research received no external funding.

Institutional Review Board Statement: Not applicable.

Informed Consent Statement: Not applicable.

Data Availability Statement: Data are contained within the article.

Acknowledgments: The authors sincerely thank Swansea Universities/UK for some chemical analysis. Also, we want to thank the Chemistry Department at Sebha University and Tripoli University/Libya for the resources and services provided.

Conflicts of Interest: Authors have declared that there was no conflict of interest.

References

1. Zhang, X.F.; Liu, Z.G.; Shen, W.; Gurunathan, S. Silver nanoparticles: Synthesis, characterization, properties, applications, and therapeutic approaches. *Int. J. Mol. Sci.* **2016**, *17*, 1534. [[CrossRef](#)] [[PubMed](#)]
2. Bruna, T.; Maldonado-Bravo, F.; Jara, P.; Caro, N. Silver nanoparticles and their antibacterial applications. *Int. J. Mol. Sci.* **2021**, *22*, 7202. [[CrossRef](#)] [[PubMed](#)]
3. Yin, I.X.; Zhang, J.; Zhao, I.S.; Mei, M.L.; Li, Q.; Chu, C.H. The antibacterial mechanism of silver nanoparticles and its application in dentistry. *Int. J. Nanomed.* **2020**, *15*, 2555. [[CrossRef](#)] [[PubMed](#)]
4. Salomoni, R.; Léo, P.; Montemor, A.F.; Rinaldi, B.G.; Rodrigues, M.F.A. Antibacterial effect of silver nanoparticles in *Pseudomonas aeruginosa*. *Nanotechnol. Sci. Appl.* **2017**, *10*, 115. [[CrossRef](#)]
5. Balkrishna, A.; Sharma, N.; Sharma, V.K.; Mishra, N.D.; Joshi, C.S. Green synthesis, characterisation and biological studies of AgNPs prepared using Shivlingi (*Bryonia laciniosa*) seed extract. *IET Nanobiotechnol.* **2018**, *12*, 371–375. [[CrossRef](#)]
6. Yamamoto, M.; Kashiwagi, Y.; Nakamoto, M. Size-controlled synthesis of monodispersed silver nanoparticles capped by long-chain alkyl carboxylates from silver carboxylate d tertiary amine. *Langmuir* **2006**, *22*, 8581–8586. [[CrossRef](#)]
7. Malhotra, S.P.K.; Alghuthaymi, M.A. Biomolecule-assisted biogenic synthesis of metallic nanoparticles. In *Agri-Waste Microbes Production of Sustainable Nanomaterials*; Elsevier: Amsterdam, The Netherlands, 2022; pp. 139–163.
8. Salem, S.S.; Fouda, A. Green synthesis of metallic nanoparticles and their prospective biotechnological applications: An overview. *Biol. Trace Elem. Res.* **2021**, *199*, 344–370. [[CrossRef](#)]
9. Vishwanath, R.; Negi, B. Conventional and green methods of synthesis of silver nanoparticles and their antimicrobial properties. *Curr. Res. Green Sustain. Chem.* **2021**, *4*, 100205. [[CrossRef](#)]
10. Candela, R.G.; Rosselli, S.; Bruno, M.; Fontana, G. A review of the phytochemistry, traditional uses and biological activities of the essential oils of genus *Teucrium*. *Planta Med.* **2021**, *87*, 432–479. [[CrossRef](#)]
11. Al-Marhaby, F.A.; Seoudi, R. Preparation and characterization of silver nanoparticles and their use in catalytic reduction of 4-Nitrophenol. *World J. Nano Sci. Eng.* **2016**, *6*, 29–37. [[CrossRef](#)]
12. Czechowska-Biskup, R.; Rokita, B.; Ulański, P.; Rosiak, J.M. Preparation of gold nanoparticles stabilized by chitosan using irradiation and sonication methods. *Prog. Chem. Appl. Chitin Its Deriv.* **2015**, *20*, 18–33. [[CrossRef](#)]
13. Mock, J.J.; Smith, D.R.; Schultz, S. Local refractive index dependence of plasmon resonance spectra from individual nanoparticles. *Nano Lett.* **2003**, *3*, 485–491. [[CrossRef](#)]
14. Mukaratirwa-Muchanyereyi, N.; Gusha, C.; Mujuru, M.; Guyo, U.; Nyoni, S. Synthesis of silver nanoparticles using plant extracts from *Erythrina abyssinica* aerial parts and assessment of their anti-bacterial and anti-oxidant activities. *Results Chem.* **2022**, *4*, 100402. [[CrossRef](#)]
15. Singh, M.; Sinha, I.; Mandal, R.K. Role of pH in the green synthesis of silver nanoparticles. *Mater. Lett.* **2009**, *63*, 425–427. [[CrossRef](#)]
16. Stankovic, M.S.; Curcic, M.G.; Zizic, J.B.; Topuzovic, M.D.; Solujic, S.R.; Markovic, S.D. *Teucrium* plant species as natural sources of novel anticancer compounds: Antiproliferative, proapoptotic and antioxidant properties. *Int. J. Mol. Sci.* **2011**, *12*, 4190–4205. [[CrossRef](#)]
17. Heuer-Jungemann, A.; Feliu, N.; Bakaimi, I.; Hamaly, M.; Alkilany, A.; Chakraborty, I.; Masood, A.; Casula, M.F.; Kostopoulou, A.; Oh, E.; et al. The role of ligands in the chemical synthesis and applications of inorganic nanoparticles. *Chem. Rev.* **2019**, *119*, 4819–4880. [[CrossRef](#)]
18. Vanlalveni, C.; Lallianrawna, S.; Biswas, A.; Selvaraj, M.; Changmai, B.; Rokhum, S.L. Green synthesis of silver nanoparticles using plant extracts and their antimicrobial activities: A review of recent literature. *RSC Adv.* **2021**, *11*, 2804–2837. [[CrossRef](#)]
19. Alqadi, M.K.; Noqtah, O.A.A.; Alzoubi, F.Y.; Alzoubi, J.; Aljarrah, K. pH effect on the aggregation of silver nanoparticles synthesized by chemical reduction. *Mater. Sci. Pol.* **2014**, *32*, 107–111. [[CrossRef](#)]
20. Molleman, B.; Hiemstra, T. Time, pH, and size dependency of silver nanoparticle dissolution: The road to equilibrium. *Environ. Sci. Nano* **2017**, *4*, 1314–1327. [[CrossRef](#)]
21. Miranda, A.; Akpobolokemi, T.; Chung, E.; Ren, G.; Raimi-Abraham, B.T. pH Alteration in Plant-Mediated Green Synthesis and Its Resultant Impact on Antimicrobial Properties of Silver Nanoparticles (AgNPs). *Antibiotics* **2022**, *11*, 1592. [[CrossRef](#)]
22. Salianni, M.; Jalal, R.; Goharshadi, E.K. Effects of pH and temperature on antibacterial activity of zinc oxide nanofluid against *E. coli* O157: H7 and *Staphylococcus aureus*. *Jundishapur J. Microbiol.* **2015**, *8*, e17115. [[CrossRef](#)]
23. Smith, D.J. Characterization of nanomaterials using transmission electron microscopy. *Nanocharakterisation* **2015**, *37*, 1–29.
24. Kouhbanani, M.A.J.; Beheshtkhoo, N.; Fotoohiardakani, G.; Hosseini-Nave, H.; Taghizadeh, S.; Amani, A.M. Green synthesis and characterization of spherical structure silver nanoparticles using wheatgrass extract. *J. Environ. Treat. Tech.* **2019**, *7*, 142–149.
25. Wang, L.; Housel, L.M.; Bock, D.C.; Abraham, A.; Dunkin, M.R.; McCarthy, A.H.; Wu, Q.; Kiss, A.; Thieme, J.; Takeuchi, E.S. Deliberate Modification of Fe₃O₄ Anode Surface Chemistry: Impact on Electrochemistry. *ACS Appl. Mater. Interfaces* **2019**, *11*, 19920–19932. [[CrossRef](#)] [[PubMed](#)]
26. Singh, P.; Mijakovic, I. Strong antimicrobial activity of silver nanoparticles obtained by the green synthesis in *Viridibacillus* sp. extracts. *Front. Microbiol.* **2022**, *13*, 820048. [[CrossRef](#)]
27. Ahmadi, M.; Adibesami, M. The effect of silver nanoparticles on wounds contaminated with *Pseudomonas aeruginosa* in mice: An experimental study. *Iran. J. Pharm. Res. IJPR* **2017**, *16*, 661.

28. Fadwa, A.O.; Alkoblan, D.K.; Mateen, A.; Albarag, A.M. Synergistic effects of zinc oxide nanoparticles and various antibiotics combination against *Pseudomonas aeruginosa* clinically isolated bacterial strains. *Saudi J. Biol. Sci.* **2021**, *28*, 928–935. [[CrossRef](#)]
29. Borcharding, J.; Baltrusaitis, J.; Chen, H.; Stebounova, L.; Wu, C.-M.; Rubasinghege, G.; Mudunkotuwa, I.A.; Caraballo, J.C.; Zabner, J.; Grassian, V.H. Iron oxide nanoparticles induce *Pseudomonas aeruginosa* growth, induce biofilm formation, and inhibit antimicrobial peptide function. *Environ. Sci. Nano* **2014**, *1*, 123–132. [[CrossRef](#)]
30. Abdussalam-Mohammed, W.; Najem, M.Y.; Errayes, A.O.; Shamsi, S.S.; Darwish, M.O.; Mezoughi, A.B. Synthesis of Highly Stabilized AuNPs Using 3, 5-Dinitrobenzoic Acid and Sodium Acetate as Capping Agents in an Aqueous Solution and their Bioactivity. *J. Nano Res.* **2021**, *70*, 67–79. [[CrossRef](#)]
31. Nayem, S.A.; Sultana, N.; Haque, M.A.; Miah, B.; Hasan, M.M.; Islam, T.; Hasan, M.M.; Awal, A.; Uddin, J.; Aziz, M.A.; et al. Green synthesis of gold and silver nanoparticles by using *amorphophallus paeoniifolius* tuber extract and evaluation of their antibacterial activity. *Molecules* **2020**, *25*, 4773. [[CrossRef](#)]
32. Usman, M.S.; Zowalaty, M.E.E.; Shameli, K.; Zainuddin, N.; Salama, M.; Ibrahim, N.A. Synthesis, characterization, and antimicrobial properties of copper nanoparticles. *Int. J. Nanomed.* **2013**, *8*, 4467–4479.

Disclaimer/Publisher's Note: The statements, opinions and data contained in all publications are solely those of the individual author(s) and contributor(s) and not of MDPI and/or the editor(s). MDPI and/or the editor(s) disclaim responsibility for any injury to people or property resulting from any ideas, methods, instructions or products referred to in the content.